Presence of a plant-like proton-translocating pyrophosphatase in a scuticociliate parasite and its role as a possible drug target

NATALIA MALLO[1], JESÚS LAMAS[2], CARLA PIAZZON[2] *and* JOSÉ M. LEIRO[1]*

[1] *Department of Microbiology and Parasitology, Laboratory of Parasitology, Institute of Research and Food Analysis, University of Santiago de Compostela, c/Constantino Candeira s/n, 15782, Santiago de Compostela, La Coruña, Spain*
[2] *Department of Cell Biology and Ecology, Faculty of Biology, University of Santiago de Compostela, La Coruña, Spain*

(*Received 29 April 2014; revised 26 June 2014; accepted 17 July 2014; first published online 14 August 2014*)

SUMMARY

The proton-translocating inorganic pyrophosphatases (H^+-PPases) are primary electrogenic H^+ pumps that derive energy from the hydrolysis of inorganic pyrophosphate (PPi). They are widely distributed among most land plants and have also been found in several species of protozoan parasites. Here we describe, for the first time, the molecular cloning and functional characterization of a gene encoding an H^+-pyrophosphatase in the protozoan scuticociliate parasite *Philasterides dicentrarchi*, which infects turbot. The predicted *P. dicentrarchi* PPase (PdPPase) consists of 587 amino acids of molecular mass 61·7 kDa and an isoelectric point of 5·0. Several motifs characteristic of plant vacuolar H^+-PPases (V–H^+-PPases) were also found in the PdPPase, which contains all the sequence motifs of the prototypical type I V–H^+-PPase from *Arabidopsis thaliana* vacuolar pyrophosphatase type I (AVP1) plant. The PdPPase has a characteristic residue that determines strict K^+-dependence, but unlike AVP1, PdPPase contains an N-terminal signal peptide (SP) sequence. Antibodies generated by vaccination of mice with a genetic or recombinant protein containing a partial sequence of the PdPPase and a common motif with the polyclonal antibody PAB_{HK} specific to AVP1 recognized a single band of about 62 kDa in western blots. These antibodies specifically stained both vacuole and the alveolar membranes of trophozoites of *P. dicentrarchi*. H^+ transport was partially inhibited by the bisphosphonate pamidronate (PAM) and completely inhibited by NaF. The bisphosphonate PAM inhibited both H^+-translocation and gene expression. PdPPase and PAM also inhibited *in vitro* growth of the ciliates. The apparent lack of V–H^+-PPases in vertebrates and the parasite sensitivity to PPI analogues may provide a molecular target for developing new drugs to control scuticociliatosis.

Key words: *Philasterides dicentrarchi*, scuticociliates, inorganic pyrophosphatase, proton pump, bisphosphonates.

INTRODUCTION

Protozoan parasites cause important emergent diseases in fish aquaculture against which very few drugs are available for treatment or prophylaxis (Woo, 1987). Thus, although scuticociliatosis caused by the amphizoic ciliate *Philasterides dicentrarchi* is a severe systemic disease that leads to high mortality in farmed turbot *Scophthalmus maximus* (Iglesias *et al*. 2001), there is as yet no effective chemotherapeutic treatment against the endoparasitic stage.

Inorganic pyrophosphate (PPi) is a critical element of cellular metabolism as it acts as both an energy donor and as an allosteric regulator of several metabolic pathways (Pace *et al*. 2011). H^+-pumping PPi (H^+-PPase) is an integral membrane protein that utilizes the energy released upon hydrolysis of PPi to transport H^+ across the membrane against the electrochemical potential gradient (Belogurov and Lahti, 2002). Two major categories of proteins that hydrolyse PPi in inorganic *ortho*-phosphate (Pi) and that play an important role in energy metabolism, thus driving many biosynthetic reactions (Kornberg, 1962), have been characterized to date: soluble and membrane-bound H^+-pumping pyrophosphatases (sPPases and H^+-PPases, respectively) (Pérez-Castiñeira *et al*. 2002*a*). These proteins are very different in both amino acid sequence and structure. The sPPases are ubiquitous proteins that hydrolyse PPi to release heat, whereas the H^+-PPases utilize the energy from PPi hydrolysis to move H^+ across biological membranes (Baltscheffsky *et al*. 1999; Pérez-Castiñeira *et al*. 2002*a*). Membrane-bound PPase activity was discovered in 1975 in homogenates from higher plants (Karlsson, 1975) and was later found to be located in plant vacuoles (Rea and Poole, 1986). H^+-PPases (EC: 3.6.1.1), also called vacuolar-type inorganic pyrophosphatases (V-PPase), are pyrophosphate-energized vacuolar membrane H^+ pumps that mediate electrogenic H^+ translocation from the cytosol to the vacuole lumen (Baykov *et al*. 1994; Pérez-Castiñeira *et al*. 2001). H^+-PPases are integral membrane proteins that were originally

* Corresponding author: Laboratorio de Parasitología, Instituto de Investigación y Análisis Alimentarios, c/ Constantino Candeira s/n, 15782, Santiago de Compostela, La Coruña, Spain. E-mail: josemanuel.leiro@usc.es

doi:10.1017/S0031182014001267

considered to be restricted to plants and certain photosynthetic bacteria (Petel and Genraud, 1989). However, they have since been identified in a wide range of organisms, including prokaryotic extremophiles and free-living and parasitic protists, such as the kinetoplastids *Trypanosoma* and *Leishmania* and the apicomplexans *Plasmodium* and *Toxoplasma* (Luo *et al*. 1999; Pérez-Castiñeira *et al*. 2002*b*; Drozdowicz *et al*. 2003; Miranda *et al*. 2008). There is clear evidence for the widespread occurrence of H^+-PPase genes in free-living ciliates such as *Paramecium tetraurelia, Histriculus caviota* and *Vorticella microstoma*, as well as in amphizoic ciliates such as *Tetrahymena pyriformis* and in parasite ciliates such as *Ichthyophthirius multifiliis* (Pérez-Castiñeira *et al*. 2002*b*); however, neither the enzymatic activity nor the cellular localization of the H^+-PPases have been characterized in these protozoa. H^+-PPases do not exist in the plasma membranes of animal hosts (Rea and Poole, 1993) and it has been demonstrated that inhibitors of these enzymes, such as PPi analogues (bisphosphonates), exert antiprotozoal effects. This enzyme may therefore be a potential target for future development of a chemotherapeutic agent against scuticociliatosis (Docampo and Moreno, 2008; Sen *et al*. 2009). Here we describe the isolation, sequence analysis, subcellular location and functional characterization of a PPase from the scuticociliate parasite *P. dicentrarchi* (PdPPase), which infects turbot. We demonstrate that *P. dicentrarchi* trophozoites possess a vacuolar and alveolar-membrane-located H^+-PPase that shares some features with other ciliates and plant enzymes and that PPi analogues inhibit the PdPPase and *in vitro* growth of this ciliate.

MATERIALS AND METHODS

Parasite and experimental animals

The I_1 isolate of the ciliate *P. dicentrarchi* (Iglesias *et al*. 2001; Budiño *et al*. 2011) was obtained from ascitic fluid of naturally infected turbot and maintained in the laboratory under the culture conditions described by Iglesias *et al*. (2003). Briefly, ciliates were cultured at 21 °C in tissue culture flasks fitted with vented caps, which allowed aeration of the complete sterile L-15 medium (Leibovitz, PAA Laboratories GmbH, 10% salinity, pH 7·2) containing 90 mg L^{-1} each of adenosine, cytidine and uridine, 150 mg L^{-1} of guanosine, 5 g L^{-1} of glucose, 400 mg L^{-1} of L-*α*-phosphatidylcholine, 200 mg L^{-1} of Tween 80, 10% of heat-inactivated fetal bovine serum (FBS) and 10 mL L^{-1} of 100× antibiotic–antimycotic solution (100 units mL^{-1} of penicillin G, 0·1 mg mL^{-1} of streptomycin sulphate and 0·25 mg mL^{-1} of amphotericin B). In order to maintain the virulence of the ciliates, fish were experimentally infected by intraperitoneal (i.p.) injection of 200 μL of sterile physiological saline containing 5×10^5 ciliates, every 6 months, and the ciliates were recovered from turbot ascitic fluid, as previously described.

Specimens of turbot *S. maximus*, of approximately 50 g body weight, were obtained from a local fish farm. The fish were maintained in 50-L closed circuit aerated seawater tanks at 17–18 °C and 30‰ salinity, and fed daily with commercial pellets. Fish were acclimatized to laboratory conditions for 2 weeks before the start of the experiments.

The mice used in the experiments were 6- to 8-week-old BALB/c mice bred from stock obtained from Harlan OLAC Ltd (Oxon, England).

All experiments were carried out in accordance with European regulations on animal protection (Directive 86/609), the Declaration of Helsinki and/or the Guide for the Care and Use of Laboratory Animals as adopted and promulgated by the US National Institutes of Health (NIH Publication No. 85-23, revised 1996). All experimental protocols were approved by the Institutional Animal Care and Use Committee of the University of Santiago de Compostela.

cDNA RACE-PCR

Total RNA was isolated with A NucleoSpin RNA kit (Macherey-Nagel, Düren, Germany) according to the manufacturer's instructions. Poly A^+ RNA was obtained from total RNA (pre-treated with DNase I, RNase Free Thermo Scientific) with a NucleoTrap mRNA mini kit (Macherey-Nagel, Düren, Germany). The RNA was purified and then analysed to estimate its quality, purity and concentration by A_{260} measurement in a NanoDrop ND-1000 Spectrophotometer (NanoDrop Technologies, USA.) The rapid amplification of cDNA ends (RACE technique was then applied to the poly A^+ RNA to obtain the full-length sequence of the gene cDNA sequence. The amplifications were carried out with a Clontech SMART™ RACE cDNA Amplification Kit (Clontech Laboratories Inc., USA) according to the manufacturer's instructions. PCR was performed with gene-specific primers designed from a partial sequence of *P. dicentrarchi* obtained from a DNA library and which show some homology with the H^+-PPase gene family (forward/reverse primer pair 5′-GATAACGCTGGAGG AATTGC-3′/5′-GACGAAGGGAGTTCCGAGG A-3′). These primers were designed and optimized by means of the Primer 3Plus program (http://www.bioinformatics.nl/cgi-bin/primer3plus/primer3plus.cgi), which is based on default parameters. The RACE PCR reaction was performed for 5 cycles for 30 s at 94 °C, 3 min at 72 °C, followed by 5 cycles for 30 s at 94 °C, 30 s at 65 °C, 3 min at 72 °C and finally 5 cycles for 30 s at 94 °C, 30 s at 68 °C and 3 min at 72 °C. The PCR products were purified from a 1%

https://doi.org/10.1017/S0031182014001267 Published online by Cambridge University Press

agarose gel in modified Tris acetate ethylenediaminetetraacetic acid (TAE) electrophoresis buffer (40 mM Tris–acetate, pH 8·0, 0·1 mM Na_2 EDTA) containing ethidium bromide (0·5 mg mL^{-1}). The DNA band was excised from the gel and purified by DNA purified with centrifugal filter devices (MicroconPCR, Millipore, USA) before being sequenced (Sistemas Genómicos, Spain).

Plasmid construction for genetic immunization

The *P. dicentrarchi* DNA was purified with the DNAesy Blood and Tissue Kit (Qiagen) before being examined to estimate its quality, purity and concentration by measurement in a NanoDrop ND-1000 Spectrophotometer (NanoDrop Technologies, USA). Partial PdPPase gene was amplified by PCR with the pair of primers designed and optimized with the Primer 3Plus program (forward/reverse; 5′-CGGGACCAGAGGTATCTTTTA-3′/5′-ATTGATGTCAACGCCCCC-3′). PCR was developed initially at 95 °C for 5 min, and then for 30 cycles of (a) 94 °C for 1 min, 55 °C for 1·5 min and 72 °C for 2 min. After completion of the 30 cycles, a 7-min extension phase at 72 °C was performed. The PCR products were purified from a 1% agarose gel in modified TAE electrophoresis buffer (40 mM Tris–acetate, pH 8·0 and 0·1 mM Na_2 EDTA) containing ethidium bromide (0·5 mg mL^{-1}). The DNA band was excised from the gel and purified by means of centrifugal filter devices (MicroconPCR, Millipore, USA) and cloned in vector pTargeT™-Mammalian Expression Vector System (Promega, USA) with the kit supplied by the manufacturer. *Escherichia coli* (strain JM109) cells were transformed and selected on the basis of ampicillin sensitivity and colour, and plasmid DNA was then extracted with Endo Free Plasmid Maxi Kit (Quiagen) following the manufacturer's instructions. The purified and cloned DNA fragment was subjected to sequence analysis and injected in mice, as described below.

Cloning, expression in pET21d vector and purification of recombinant protein

The *P. dicentrarchi* mRNA was extracted (from 5×10^6 ciliates) with the NucleoTrap mRNA Mini Kit (Macherey-Nagel, Germany) according to the manufacturer's instruction. Partial PdPPase gene was amplified by RT-PCR with the forward 5′-CCCGAATTCCGGGACCAGAGGTATCTTTTA-3′ (*Eco*RI) and the reverse primer 5′-AAGGGGGCGTTGACATCAATGCGGCCGCAAA-3′ (*Not*I). The PCR-purified product was cloned in pET-21d expression vector and transformed into *E. coli* DH5α cells as in the standard protocol. This construct was transformed into *E. coli* BL21 (DE3) cells. The positive clone was confirmed by nucleotide sequencing. The logarithmic phase cultures were induced with different concentrations of isopropyl thiogalactoside (IPTG) (0·5, 1, 1·5 and 2 mmol L^{-1}) in Luria Bertani (LB) media and checked at hourly intervals for a period of 5 h. The cell suspension was sonicated and the resultant cell lysate was centrifuged at 11 000 ***g*** for 15 min at 4 °C to identify the location of the recombinant protein. The clear supernatant and remaining pellet were collected separately and analysed by 12·5% sodium dodecyl sulphate (SDS)-PAGE.

Recombinant clone in BL21 (DE3) cells was induced with 1 mM IPTG at 37 °C for 7 h in LB containing 50 μg mL^{-1} ampicillin. When the OD_{600} of the culture reached approximately 0·6, the cell pellet was suspended in 5 mL of cell lysis buffer MCAC-0 (20 mM Tris–HCl pH 7·9, 0·5 M NaCl, 10% v/v glycerol and 1 mM phenylmethanesulphonyl (PMSF)) and 50 mL of 100× protease inhibitor cocktail (Promega). The sample was initially sonicated for 3 cycles of 5 pulses of 1 min at 60 W and was then subjected to 3 cycles of freezing at −70 °C and thawing on ice before 0·05 mL of 1 M $MgCl_2$ and 0·05 mL of DNaseI solution was added. The sample was then incubated for 10 min at room temperature and centrifuged for 30 min at 11 000 ***g*** at 4 °C, and the resulting supernatant was analysed by SDS-PAGE. The recombinant protein was purified by immobilized metal affinity chromatography on a precharged Ni Sepharose Histrap column (ÄKTAprime plus, GE Healthcare Life Sciences). The column was initially equilibrated with 5 mL of binding buffer (20 mM sodium phosphate, 0·5 M NaCl, 20 mM imidazole, pH 7·4). Finally, the protein bound to the column was eluted in 15 mL of elution buffer (20 mM sodium phosphate, 0·5 M NaCl, 250 mM imidazole, pH 7·4). Each elute was collected in 1-mL fractions and analysed by 12·5% SDS-PAGE. The fractions of purified protein were pooled and dialysed overnight in 2 L of bidistilled water. The dialysed sample was concentrated to 150 mL in an Amicon Ultra centrifugal filter device (Millipore, USA) with a 10-kDa cut-off membrane. The final protein concentration was estimated by the Bio-Rad Protein Assay, which is based on the Bradford assay (Bradford, 1976).

Immunization and serum extraction

For the genetic immunization, a group of 5 BALB/c mice were anaesthetized by i.p. injection with 30 μL of a mixture of 5 mL of 100 mg mL^{-1} ketamine and 1 mL of 20 mg mL^{-1} xylazine. A 50 μL saline solution (0·9% NaCl, sterile) containing 50 μg of pure plasmids, and 50 μL of saline containing 0·4% trypan blue, was then injected in the quadriceps muscle at a point 0·5 cm above the knee, 0·2 cm deep and at an angle of 30°, with the aid of a tuberculin syringe fitted

https://doi.org/10.1017/S0031182014001267 Published online by Cambridge University Press

with a 28 G needle (Becton Dickinson, USA). After 30 days, the mice were re-immunized with the same dose of plasmids.

To obtain antibodies against recombinant protein, another 5 BALB/c mice were intraperitoneally injected with a saline solution (0·9% NaCl, sterile) containing 66 μg of purified PdPPase in an emulsion prepared with complete Freund's adjuvant. After 30 days, mice were re-immunized with the same quantity of PdPPase, but with incomplete Freund's adjuvant.

Sixty days after the first injection, mice were bled via the retrobulbar venous plexus. The blood was left to coagulate overnight at 4 °C before the serum was separated by centrifugation (2000 ***g*** for 10 min), mixed 1:1 with glycerol and stored at −30 °C until use (Leiro *et al*. 2002).

SDS-PAGE and immunoblotting

For polypeptide analysis of total proteins, 3×10^6 ciliates were resuspended in 100 μL of reduction buffer (62 mM Tris–HCl buffer, pH 6·8, containing 2% SDS, 10% glycerol and 0·02 M dithiothreitol (DTT) and 1 mM PMSF) and were denatured by incubation for 5 min at 100 °C. Total proteins and recombinant proteins were separated on 12·5% linear gels by SDS-PAGE (Piazzón *et al*. 2008). The gels were first electrophoresed and then stained with Thermo Scientific GelCode Blue Safe Protein Stain (Thermo Fisher, USA) for qualitative determination of the protein concentration in each sample. At the same time, 1 gel was immunoblotted at 15 V for 35 min to Immobilon-P transfer membranes (0·45 mm; Millipore, USA) in a trans-blot SD transfer cell (Bio-Rad, USA) with the electrode buffer containing 48 mM Tris, 29 mM glycine, 0·037% SDS, 20% methanol and pH 9·2. Membranes were washed with Tris buffer saline (TBS; 50 mM Tris, 0·15 M NaCl and pH 7·4) and stained with Ponceau S, to verify transfer, blocked for 2 h at room temperature with TBS containing 0·2% Tween 20 and 5% non-fat dry milk, then washed in TBS and incubated for overnight at 4 °C with the different antibodies (mouse anti-PPase at 1:50 dilution, anti-T7-Tag at 1:10 000 dilution). The membranes were washed with TBS and incubated for 1 h at room temperature with peroxidase-conjugated goat anti-mouse immunoglobulin (Ig) (Dakopatts; dilution 1:1000) before being visualized with enhanced luminol-based chemiluminiscent substrate (Pierce ECL Western Blotting Substrate, Thermo Scientific, USA) and photographed with a FlourChem® FC2 imaging system (Alpha Innotech, USA).

Phylogenetic analyses

The sequences obtained for the PdPPase gene were aligned with CLUSTAL Omega software (Sievers *et al*. 2011) and edited with the Jalview Multiple Alignment Editor (V1.8). Sites containing gaps were excluded. Phylogenetic trees were constructed with MEGA 5 (Tamura *et al*. 2011), and the neighbour-joining (NJ) method was applied to Kimura 2-parameter distances. Confidence estimates were obtained on the basis of bootstrap generation of 1000 trees.

Immunolocalization

An aliquot of 5×10^6 ciliates was centrifuged at 700 ***g*** for 5 min, washed twice with phosphate buffered saline (PBS) and fixed overnight a 4 °C in a solution of 5% formaldehyde in PBS. The ciliates were then washed twice with PBS, resuspended in a solution of 30% sucrose and mounted on thin cardboard in OCT embedding medium (Miles Laboratories, USA). Cryostat sections of thickness 12 μm were cut at −25 °C on slides, dried and left at 4 °C overnight to obtain good fixation to the glass slide. After 1 h at room temperature, the sections were washed 3 times for 5 min with gentle shaking followed by a 10 min wash with PBS containing 0·2% Triton X-100 (PBT). Sections were blocked in darkness with PBT containing 3% bovine serum albumin (BSA) and 0·5% H_2O_2, for endogenous peroxidase blockade, during 20 min. After blocking, sections were washed 3 times with PBT for 5 min and incubated at 4 °C overnight with a solution containing 3% BSA, 15% normal rabbit serum and a 1:100 dilution of anti-PdPPase mouse serum. The sections were then washed 3 times with PBT followed by incubation for 2 h at room temperature with a 1:500 dilution of rabbit anti-mouse Igs conjugated with peroxidase (Dako, Denmark) prepared in PBT containing 3% normal rabbit serum and 3% BSA. A developing solution of diaminobenzidine (DAB, SIGMAFAST™ 3,3′-diaminobenzidine; Sigma) containing 0·01% H_2O_2 was then added and the sections were incubated for 10 min at room temperature. Finally, the sections were dehydrated in ethanol, immersed in xylene and mounted in Entellan® (Merck Millipore).

Reverse transcription-quantitative real-time polymerase chain reaction (RT-qPCR)

Total RNA was isolated with a NucleoSpin RNA kit (Macherey-Nagel, Düren, Germany) according to the manufacturer's instructions. The RNA was purified and then analysed to estimate the quality, purity and concentration by A_{260} measurement in a NanoDrop ND-1000 Spectrophotometer (NanoDrop Technologies, USA.). cDNA synthesis (25 μL per reaction mixture) was achieved with 1·25 μM random hexamer primers (Roche), 250 μM each deoxynucleoside triphosphate (dNTP), 10 mM

https://doi.org/10.1017/S0031182014001267 Published online by Cambridge University Press

DTT, 20 U of RNase inhibitor, 2·5 mM $MgCl_2$, 200 U of Moloney murine leukaemia virus reverse transcriptase (Promega) in 30 mM Tris and 20 mM KCl (pH 8·3), and 2 μg of sample RNA. PCR was performed with gene-specific primers for the PdPPase gene (forward/reverse primer pair 5′-GC CTACGAAATGGTCGAAGA-3′/5′-GCATC GGTGTATTGTCCAGA-3′) (accession number KF135294). A parallel PCR with primers for the β-tubulin gene (forward/reverse primer pair, 5′-AC CGGGGAATCTTAAACAGG-3′/5′-GCCACC TTATCCGTCCACTA-3′) (accession number GQ342956) was used as a reference gene for RT-qPCR. Primer sets were designed and optimized with the Primer 3Plus program on the basis of default parameters. PCR mixtures (20 μL) contained 10-μL Maxima SYBR green qPCR Master Mix (Thermo Scientific), the primer pair at 300 nM, 1 μL of cDNA and RNase–DNase-free water. PCR mixtures were heated to 95 °C for 5 min, followed by 40 cycles at 95 °C for 10 s and 60 °C for 30 s. This was followed by melting-curve analysis at 95 °C for 15 s, 55 °C for 15 s and 95 °C for 15 s. The specificity and size of PCR products for each gene were confirmed by gel electrophoresis. All PCRs were performed in an Eco Real-Time PCR system (Illumina). Relative quantification of gene expression was determined by the $2^{-\Delta\Delta Cq}$ method (Livak and Schmittgen, 2001) with software conforming to minimum information for publication of quantitative real-time PCR experiments guidelines (Bustin *et al*. 2009).

Measurement of PPi-dependent H^+-translocation

PdPPase-driven H^+ transport was assayed by means of a fluorimetric assay with acridine orange as transmembrane pH difference indicator in the assay medium containing vacuole-enriched fractions. Trophozoites ($2{\cdot}5 \times 10^5$ cells for each preparation) were centrifuged and washed twice in PBS and once with assay buffer (100 mM KCl, 0·4 M glycerol, 1 mM Tris–EGTA and 5 mM Tris–HCL, pH 8·0) containing 1 mM PMSF and 1 μg mL^{-1} leupeptin. The cell pellet was homogenized in a Homogenizer PotterS (Braum Biotech, USA) until lysis was greater than 90% (generally 30 s). The mixture was resuspended in 5 mL of assay buffer and centrifuged once at 750 ***g*** for 5 min (to remove unbroken cells). The resulting supernatant was centrifuged at 15 000 ***g*** for 10 min, and the pellet was resuspended in 1 mL of assay buffer containing 2·5 μM acridine orange. Reaction was initiated by the addition of Tris–PPi (1 mM) to media containing $MgSO_4$ (1·3 mM) in the case of V-PPase-mediated H^+ translocation. The decrease in fluorescence was measured at excitation and emission wavelengths of 485 and 530 nm, respectively (Rui-Guang Zhen *et al*. 1997; Hill *et al*. 2000; Marchesini *et al*. 2000; Rodrigues *et al*. 2000).

Prior to the H^+-translocation assay, an immunofluorescence assay was performed with anti-recombinant vacuolar PdPPase antibodies, to verify that the above-mentioned fraction was enriched in vacuoles of the ciliate. Briefly, the cellular fraction obtained was blocked for 30 min in 1% BSA in PBS at room temperature. The anti-PPase antibody, diluted 1:100 in dilution buffer containing 1% BSA, 0·05% Triton X-100 in PBS, was then added and the samples were incubated for 1 h at room temperature. After 3 washes with PBS, a rabbit anti-mouse IgG-FITC antibody (Sigma) (diluted 1:80 in dilution buffer) was added. After incubation for 1 h at room temperature and 3 washes in PBS, the samples were mounted in PBS–glycerol (1:1) and visualized under a fluorescent microscope (Zeiss Axioplan, Germany).

In vitro *growth assay*

The effects of sodium pamidronate (PAM; Sigma-Aldrich) on the *in vitro* growth of *P. dicentrarchi* were determined as previously described, with minor modifications (Leiro *et al*. 2004). A stock solution of PAM was prepared in distilled water, to a concentration of 100 mM, and stored at 4 °C. In order to investigate the effects on *P. dicentrarchi*, PAM was added to wells of sterile 12-well culture plates (Corning) containing 1×10^4 trophozoites per well in 1 mL of L-15 medium (Leibovitz, PAA Laboratories GmbH, 10% salinity, pH 7·2) with different concentrations of PAM (25, 50 and 100 μM). Control wells without PAM were included. The plates were incubated for 3 days at 20 °C. The number of ciliates was determined daily by counting the numbers in 10-μL aliquots of the medium removed from each well, in a haemocytometer.

Bioinformatic and statistical analysis

Identification of protein domains and protein functional analysis was performed with the InterProScan tool (version 4.8) of the European Bioinformatics Institute (EMBL-EBI), available at http://www.ebi.ac.uk/Tools/pfa/iprscan/ (Zdobnov and Apweiler, 2001; Quevillon *et al*. 2005). PPase modelling was performed with the Swiss-model server, accessible via the ExPASy web server, or the Deep View program (Swiss PDB-Viewer), available at http://swissmodel.expasy.org/ (Kiefer *et al*. 2009). The physicochemical properties of the PPase were determined from the amino acids (aa) sequence, with the ProtParam bioinformatics tool of the ExPASy server, available at http://web.expasy.org/tools/protparam/. The phosphorylation sites in the protein were predicted with NetPhos Server 2.0, available at http://www.cbs.dtu.dk/services/NetPhos/. The presence and location of SP cleavage sites in amino acid sequences were predicted with the Signal-3L

https://doi.org/10.1017/S0031182014001267 Published online by Cambridge University Press

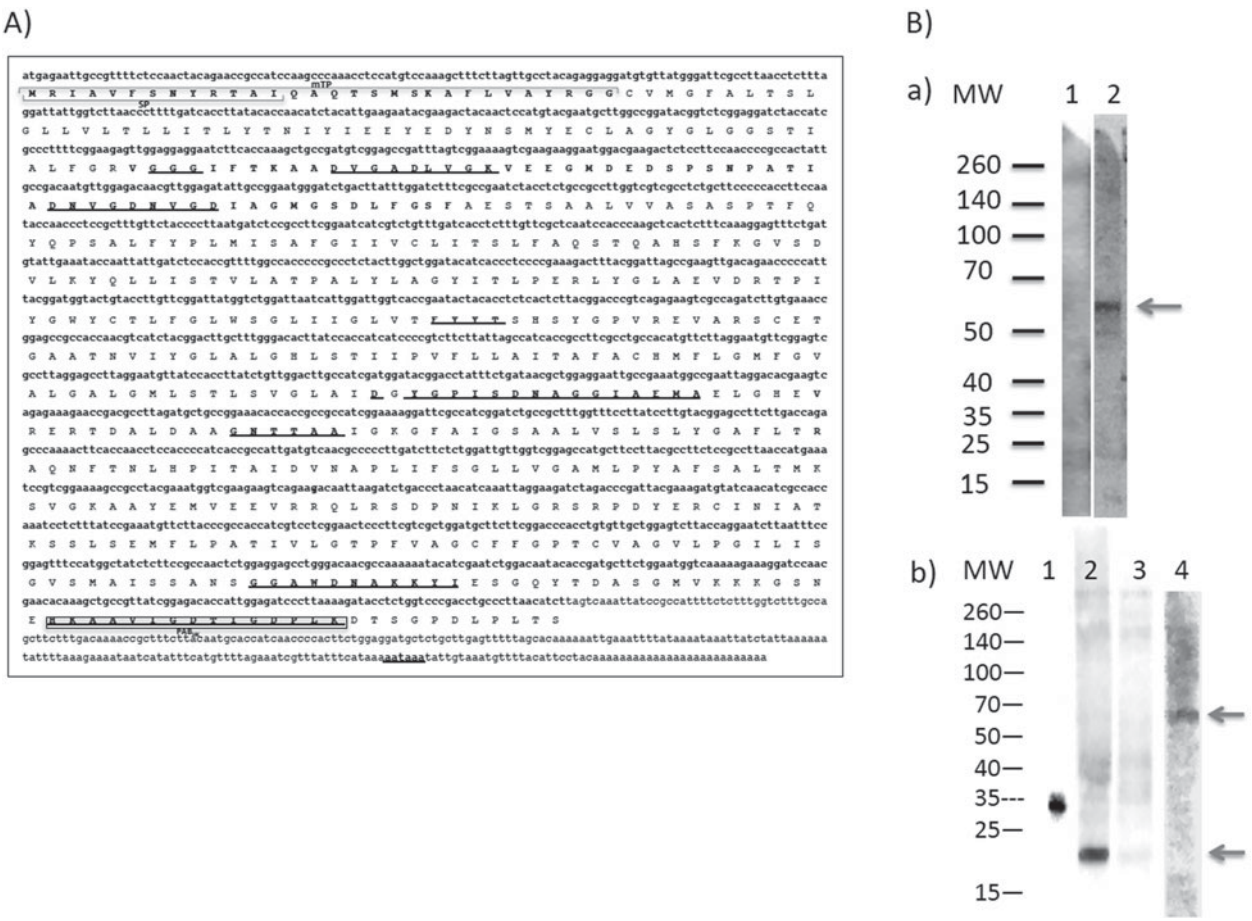

Fig. 1. (A) Nucleotide sequence and translation of the amino acid sequence of cDNA corresponding to the PdPPase in which the nucleotidic bases highlighted in bold type correspond to the ORF. The 15 initial aa function as a SP, and the 30 initial aa correspond to a mTP predicted by Signal-3L and iPSORT, respectively. In the third and fourth row, the residue of 57 aa containing 3 motifs (underlined) typical of all H^+-PPases is indicated in bold type. In the tenth row of the sequence, a highly conserved GNTAAA domain containing the A form (asterisk), related to K^+ dependence, is indicated in bold type and underlined. In lines 7, 10 and 14, the conservative sequences predicted for the archetypal V-PPase type 1 of AVP1 are indicated in bold type and underlined. Conserved epitopes for polyclonal antibody PAB_{HK} are included within the box. (B) Immunorecognition pattern identified by western blot with (a) antibodies generated by intramuscular immunization with the plasmid pTargetT (lane 1) and with the plasmid pTarget T containing a fragment of DNA of 531 bp, located between positions 1233 and 1764 of the nucleotide sequence of the PdPPase (lane 2) on total proteins from *P. dicentrarchi*, and with (b) a polyclonal antibody anti-recombinant PdPPase: lane 1: T7-tagged *β*-galactosidase fusion protein; lane 2: total extracts of *E. coli* expressing the T7-tag fusion protein; lane 3: total extracts of *E. coli* expressing the T7-tag fusion protein faced with a normal mouse serum; lane 4: total *P. dicentrarchi* proteins. The arrow indicates the band corresponding to the PdPPase. Mw: molecular weight markers in kDa.

server, available at http://www.csbio.sjtu.edu.cn/bioinf/Signal-3L/ (Shen and Chou, 2007). The N-glycosylation sites were predicted with the NetNglyc server (http://www.cbs.dtu.dk/services/NetNGlyc/). The iPSORT bioinformatics tool, available at http://ipsort.hgc.jp/, was used to determine whether the aa sequence of PPase contains a mitochondrial targeting peptide (mTP). The transmembrane helix domains in the protein were predicted with the THHMM server, v 2.0, available at http://www.cbs.dtu.dk/services/TMHMM-2.0/.

The data shown in the figures are expressed as means ± S.E.. The statistical significance ($P = 0{\cdot}05$) of any differences was determined by 1-way analysis of variance followed by the Tukey–Kramer test for multiple comparisons.

RESULTS

Identification of cDNA encoding PdPPase

We initially constructed a plasmid DNA library for *P. dicentrarchi* and after sequencing the clones and using BLAST to compare the sequences with those reported in existing databases, we found a sequence that showed high homology with the H^+-PPase gene; however, the clone only contained a partial gene sequence. We then designed a pair of primers in a defined internal site and used the RACE technique to obtain full-length cDNA from the mRNA template (Fig. 1). The full-length cDNA was 2031 bp with an open reading frame (ORF) of 1761 bp (Fig. 1A), which contained the ATG initiation codon and ended with 26-bp poly(A)$^+$ tail that began 25-bp

https://doi.org/10.1017/S0031182014001267 Published online by Cambridge University Press

downstream of the sequence AATAAA, which is the eukaryotic consensus polyadenylation signal (Fig. 1A).

Protein sequence characteristics

The entire ORF of the PdPPase cDNA encodes a sequence of 587 amino acids, predicting a 61 666-Da polypeptide with an isoelectric point of 5·0. Predictions obtained with the NetPhos 2.0 server for serine, threonine and tyrosine phosphorylation sites indicate that the protein has 19 phosphorylation sites in Ser, 5 in Thr and 10 in Tyr. Two potential sites for N-glycosylation (372 and 403 sites) were predicted in the protein. According to the Signal-3L program, the protein contains a SP at positions 1–15 and a mTP at position 1–30 (iPSORT prediction, Fig. 1A). The protein sequence contains a 57-aminoacidresidue loop with 3 H^+-PPase characteristic sequence motifs, underlined in the following sequence, at positions 86–143:V**GGG**IFTKAA-**DVGADLVGK**VEEGMDEDSPSNPATIA**DNVG-DNVGD**IAGMGSDLFGSF (Fig. 1A). The T (acidid) YYT (neutral) motif containing aa neutral E and acid S, typical of the type I K^+-dependent V-PPase, occurred at positions 260–265 (Fig. 1A). Membership of the family of K^+-dependent V-PPases is also supported by the presence of an alanine (A) at position 375, which determines strict K^+-dependence (Fig. 1A). A search for members of the membrane-bound, H^+ pumping H^+-PPase family was carried out using the information obtained from InterPro Scan of EMBL, EBI, a bioinformatics tool designed for functional analysis of proteins. We found that the protein sequence shared a high degree of sequence similarity with the family of proteins pyrophosphatase-energized H^+ pump, between nucleotides 1 and 583 (according to the search method PFAM of the Sanger Institute), with a match of 6·9E-223. A similarity of 3·5E-227 was identified by a search in the Comprehensive Microbial Resource database. All sequence motifs and residues that are characteristic of type I V-PPases are conserved in PdPPase. The protein has 4 motifs characteristic of *Arabidopsis* vacuolar pyrophosphatase type I (AVP1): the EYYTS motif located between sites 260 and 265; the DG(A)YGPISDNAGGIAEMA motif located between sites 338 and 354, which has a single substitution of glycine (Gly) by alanine (Ala) at position 2; the GGAWDNAKKYIE motif located between sites 532 and 543 and the HKAAVI-GDTIGDPLKDT motif located between sites 562 and 578 (Fig. 1A). The topological model of the PdPPase, predicted by the THHMM program, indicates that the protein has 11 transmembrane helix regions located between sites 35 and 57, 70 and 92, 165 and 187, 206 and 225, 240 and 262, 286 and 308, 313 and 335, 380 and 402, 417 and 439, 484 and 506, 510 and 532, located in the second loop in the PdPPase binding domain.

For characterization of the PdPPase, we proceeded to generate mouse antibodies obtained by genetic immunization with a DNA fragment and by immunization with the recombinant protein fragment of the PdPPase. The plasmid construction used for genetic immunization was a DNA fragment of 531 bp cloned into the eukaryotic expression vector pTargeT. The recombinant protein was performed by plasmid construction with DNA fragment of 507 bp in the pET-21d vector, encoding a protein of 169 aa residues located between 413 and 582 of the PdPPase sequence. In a western blot of total protein of *P. dicentrarchi*, the antibodies produced by the genetic immunization procedure recognized a single band of approximately 60 kDa (Fig. 1B, a). For the recombinant protein, we also performed a western blot assay with total bacterial extracts and the monoclonal anti-T7-Tag that recognizes a single band of around 20 kDa, which corresponds to the predicted size of the originally designed recombinant protein including an additional vector peptide of 14 aa containing a His tag (Fig. 1B, b). The serum from immunized mice recognized a single band of approximately 60 kDa (Fig. 1B, b).

Phylogenetic analysis

For comparison of ciliate H^+-PPases (*Tetrahymena thermophila, P. tetraurelia, I. multifiliis* and *P. dicentrarchi*), we performed multiple sequence alignments and analysed 5 conserved segments (CS) characteristic of V-PPases from *Arabidopsis* (AVP1 and AVP2), *Rhodospiriullum rubrum* (RVP) and from *Pyrobaculum aerophilum* (PVP) (Fig. 2A). The PdPPase presents identical AVP1 residues in CS2 (the EYYTS motif), in CS4 (the GGAWDNAK-KYIE motif) and in CS5 (the HKAAVIGD-TIGDPLKDT motif); however, it differs from AVP1 in residues corresponding to CS1 and by only 1 change in CS3 (Ala/Gly) (Fig. 2A). The H^+-PPases of the other ciliates analysed also exhibit the same AVP1 sequence pattern in most CS, except in CS3 and CS5, in which the sequence patterns are types PVP and RVP, respectively (Fig. 2A). Comparison of ciliate H^+-PPases revealed that the PdPPase was most similar to the H^+-PPase of *T. thermophila* (73%), followed by the H^+-PPase of *I. multifiliis* (71%) and the H^+-PPase of *P. tetraurelia* (69%) (Fig. 2B). The phylogenetic tree constructed by the NJ method revealed that ciliate H^+-PPases represent a related but different group from plant PPases. Within the ciliate subgroup, the H^+-PPases of *T. thermophila* and *I. multifiliis* are more closely clustered, whereas H^+-PPases of *P. dicentrarchi* and *P. tetraurelia* are phylogenetically more distant (Fig. 2C).

https://doi.org/10.1017/S0031182014001267 Published online by Cambridge University Press

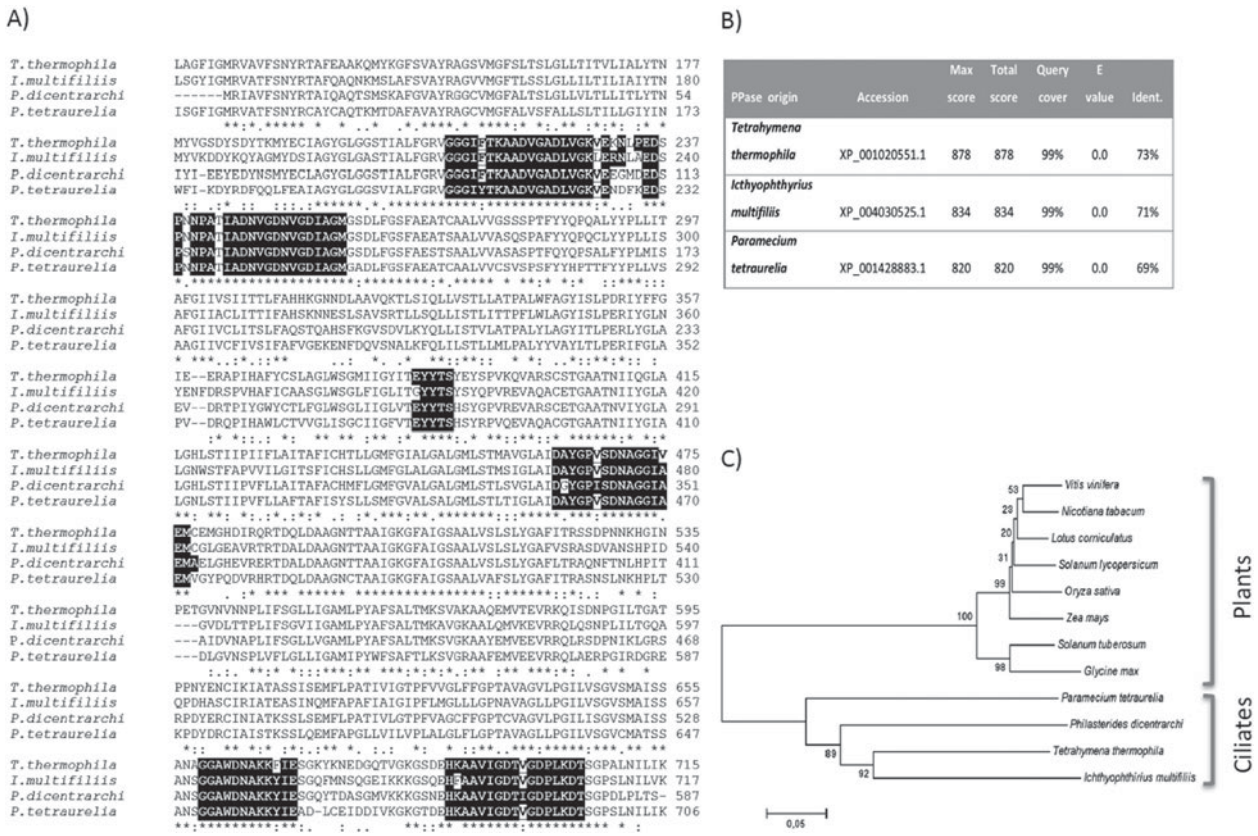

Fig. 2. (A) ClustalW2 multiple amino acid sequence alignment of H^+-PPases of ciliates *P. dicentrarchi, I. multifiliis, T. thermophila* and *P. tetraurelia*. Identical residues among sequences are marked with asterisks. Dashes indicate gaps inserted to optimize the alignments. Five toolbox sequences with the greatest conservation among AVP1 are included: identical residues are shown as white letters on a black background. (B) Ciliate species included in the phylogenetic analysis, showing GenBank accession numbers for their amino acid sequences, and percentage of identity with the PPase amino acid sequence from *P. dicentrarchi*. (C) Phylogenetic tree of aligned amino acid sequences of H^+-PPase of *P. dicentrarchi* and other species of ciliates and plants. The phylogeny presented is based on alignments of protein sequences identified by the ClustalW2 program for multiple sequence alignment. An NJ phylogenetic tree was constructed with MEGA 5. The numbers at the nodes represent bootstrap values out of 1000 resampled values in the NJ analysis with the Kimura 2-parameter correction mode. Scale bar indicates a distance of 0·05.

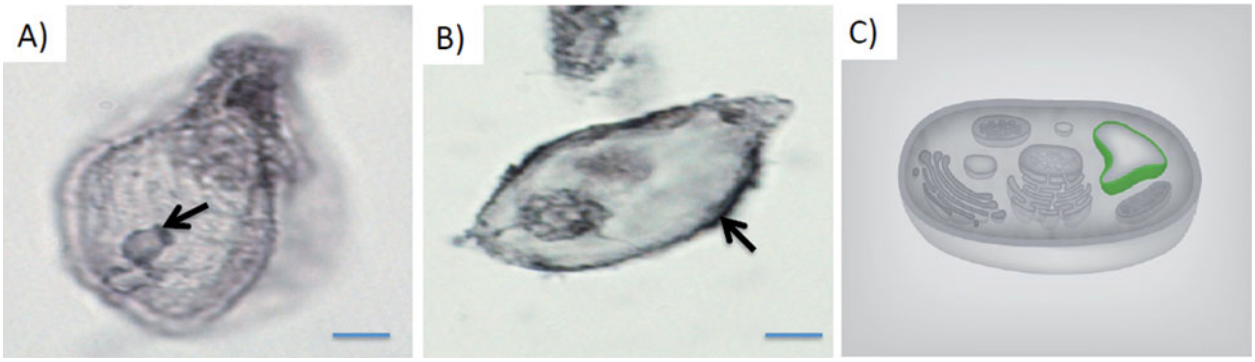

Fig. 3. Immunolocalization of H^+-PPase of *P. dicentrarchi* (PdPPase). The cellular location of the PdPPase was identified by immunohistochemistry with a recombinant polyclonal antibody anti-PdPPase (see Fig. 4). Staining of anti-PdPPase antibody on the vacuole membrane (A) and alveolar membranes (B). Prediction of the location of the sequence of the PdPPase by use of the LocTree2 bioinformatics tool (C). Scale bar = 10 μm.

Subcellular localization of PdPPase

To confirm the subcellular location of PdPPase, we analysed the *P. dicentrarchi* trophozoites using antibodies against the recombinant protein fragment of the PdPPase (see the previous section). The anti-PdPPase produced intense staining of membrane vacuoles (Fig. 3A) and the alveolar membranes (Fig. 3B) of trophozoites. The subcellular localization identified by use of anti-PdPPase in

https://doi.org/10.1017/S0031182014001267 Published online by Cambridge University Press

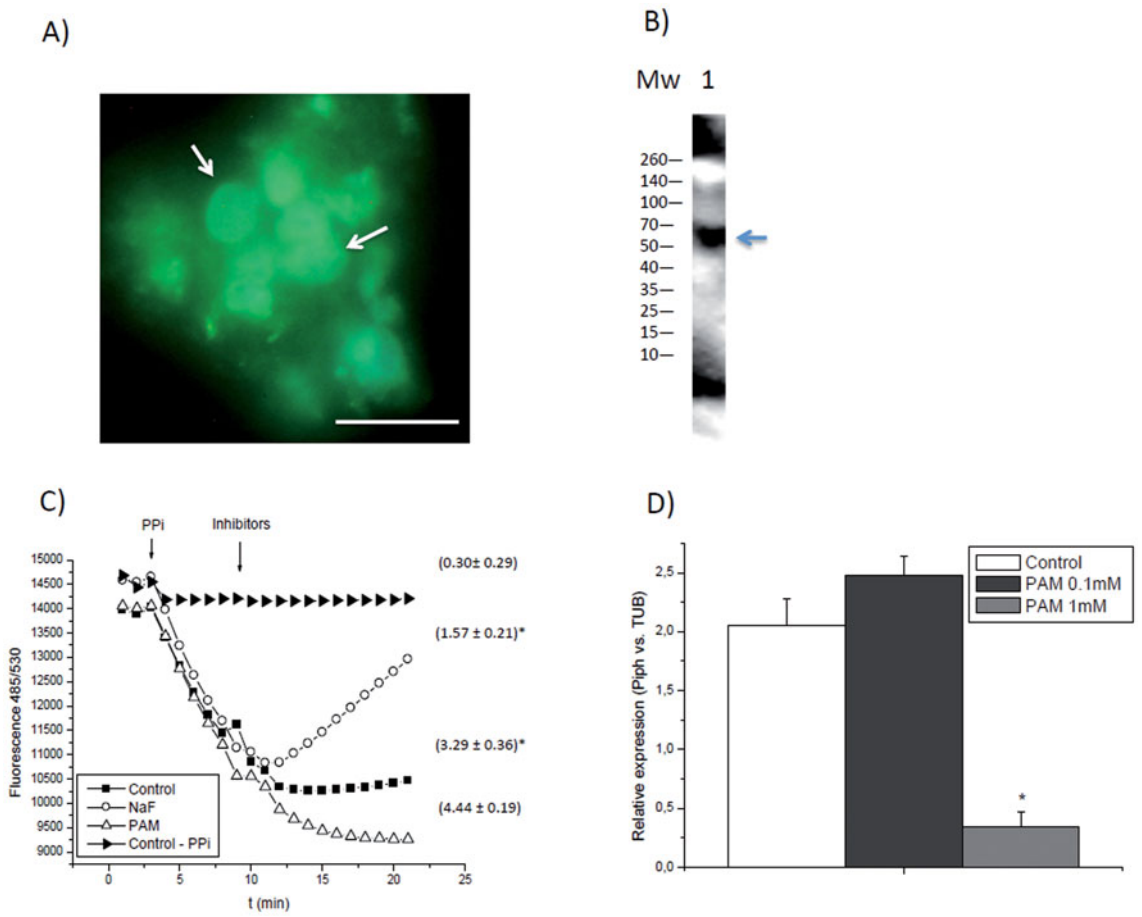

Fig. 4. (A) Photomicrograph of indirect immunofluorescence with anti-PdPPase recombinant antibodies on a vacuole-enriched fraction of *P. dicentrarchi* trophozites (arrows show FITC-labelled vacuoles present in this fraction). Scale bar = 5 μm. (B) Western blot of polyclonal anti-recombinant PdPPase on vacuole-enriched fractions: the arrow indicates the band corresponding to the PdPPase. (C) PPi-dependent H^+ translocation assayed on vacuole-enriched fraction with the fluorescent *ΔpH*, acridine orange, in the presence of enzyme inhibitors NaF at 1 mM and the PPi analogue bisphosphonate PAM at 0·1 mM. (D) Relative gene expression levels of PdPPase determined by RT-qPCR in the presence of PPi analogue PAM, at the concentrations shown. Gene expression was normalized to the reference gene β-tubulin of *P. dicentrarchi* and normalized data are expressed in arbitrary units. Values shown are mean values ± S.E. (n = 5 assays). *P < 0·01 relative to the control.

immunohistochemical assays is also consistent with the protein cellular localization predicted by use of the LocTree2 program (Fig. 3C).

Effect of NAF and bisphosphonates on PPi-dependent H^+-translocation and gene expression

For measurement of PPi-dependent H^+-translocation, we used a vacuole-enriched fraction of *P. dicentrarchi* trophozites known to contain large amounts of this enzyme, as demonstrated by immunofluorescence (Fig. 4A) and by a western blot (Fig. 4B) with antibodies against the recombinant vacuolar PdPPase. PPi hydrolysis and PPi-induced acidification in vacuole-enriched fractions of *P dicentrarchi* trophozoites were monitored with acridine orange in the medium containing 1 mM NaF and 0·1 mM PAM, the PPi analogue (Fig. 4C). We have previously observed that in the absence of PPi in the reaction medium, the fluorescence values are not altered and therefore the acidification of the vacuole pattern recognition is not altered; however, in the present study the addition of PPi to the reaction mixture caused a significant decrease in fluorescence, indicating an increase in the acidification of the vacuoles (Fig. 4C). Addition of NaF and PAM to the reaction medium after stimulation with PPi significantly inhibited acidification of vacuoles, relative to the controls (Fig. 4C), but did not affect the fluorescence levels in the assays in which PPi was not added to the incubation medium. We also used RT-qPCR to analyse the effect of bisphosphonates on PdPPase gene expression and observed that 1 mM PAM significantly inhibited PdPPase expression, relative to untreated controls (Fig. 4D).

Effect of PdP Pase inhibitors on in vitro *cell growth*

Finally, we analysed the effect of the PdPPase inhibitor bisphosphonate PAM on the *in vitro* growth

https://doi.org/10.1017/S0031182014001267 Published online by Cambridge University Press

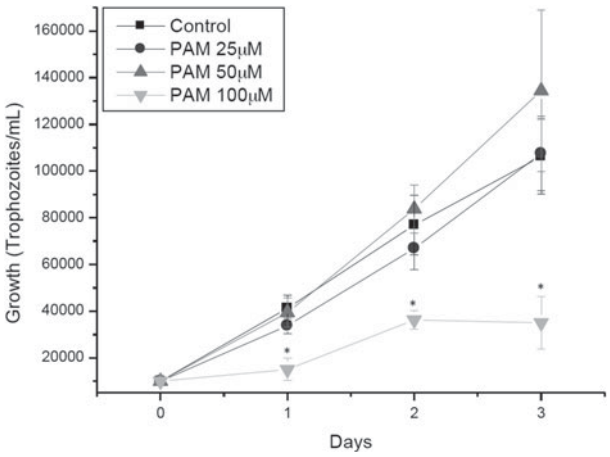

Fig. 5. Effect of bisphosphonate PAM, at concentrations of 25, 50 and 100 μM, on the *in vitro* growth of *P. dicentrarchi* in complete L-15 medium for 3 days. Values shown are mean values ± S.E. ($n = 5$ assays) of the number of trophozoites per mL. *$P < 0{\cdot}01$ relative to the control.

of *P. dicentrarchi* (Fig. 5). Addition of 100 μM PAM caused significant inhibition of *in vitro* growth from day 1 onwards (Fig. 5).

DISCUSSION

The findings reported here constitute the first molecular and functional characterization of a type I V-PPase derived from the scuticociliate parasite *P. dicentrarchi*. We have established that this ciliate has a PPi-dependent H^+ pump that bears a close resemblance to the canonical type I V-PPases from plants. PPases are essential for growth and viability in various organisms including parasites (McIntosh *et al*. 2001; Islam *et al*. 2005), and they are attractive targets for the development of new chemotherapeutic drugs and vaccines against parasitic infections (Xie *et al*. 2013). The H^+-PPase is a unique electrogenic H^+ pump that is distributed among most land plants but only present in some alga, yeasts, protozoa, phototrophic bacteria and archeobacteria (Rea and Poole, 1993; Scott *et al*. 1998; Rodrigues *et al*. 1999*a*, *b*; Maeshima, 2000). Native H^+-PPases are divided into 2 types (types I and II) depending on whether they are K^+-dependent or K^+-independent and on whether their activity is sensitive to inhibition by Ca^{2+} (Gaxiola *et al*. 2007; Wang *et al*. 2013). Most K^+-independent H^+-PPases have been identified in eukaryotes, bacteria and archaea, whereas K^+-dependent H^+-PPases have only been identified in eukaryotes (Pérez-Castiñeira *et al*. 2001). Proteins of all members of the gene family of types I and II H^+-PPases are characterized by the presence of a 57 amino acid residue loop that contains 3 sequence motifs: GGG, DVGADLVGK and DNVGDNVGD, which are important from an evolutionary point of view and also appear to have a functional role as part of the active site of the enzyme (Baltscheffsky *et al*. 1999; Nakanishi *et al*. 2001; Drozdowicz and Rea, 2001; Hedlund *et al*. 2006; Serrano *et al*. 2007). In the amino acid sequence of the *P. dicentrarchi* PdPPase, 2 additional domains are also typical: EYYT and GNTTAA motifs, which have been described as specific to the H^+-PPase family (Drozdowicz and Rea, 2001; Hedlund *et al*. 2006). These motifs may be related to Mg^{2+}-PPi binding, PPi hydrolysis and energy transfer (Gaxiola *et al*. 2007). The triglycyl sequence occurs in all H^+-PPase family members and may be expected to have the potential to provide unusually high local conformational change (Baltscheffsky *et al*. 1999). The GGG sequence has also been used as a spacer to allow mimicking of the swing of the lever arm of a myosin motor (Suzuki *et al*. 1998). It has been proposed that the (E/D)(X_7)KXE configuration is a catalytic site of the H^+-PPases (Rea *et al*. 1992*a*; Rea and Poole, 1993), the sequence corresponding to DVGADLVGKVE located in the hydrophilic loop and the carboxyl terminal part of H^+-PPase of *P. dicentrarchi* in this configuration. It has also been suggested that this motif may participate directly in substrate and Mg^{2+} binding (Cooperman *et al*. 1992; Rea and Poole, 1993; Takasu *et al*. 1997; Baykov *et al*. 1999). The second and third motifs, DVGADLVGK and DNVGDNVGD, may be involved in substrate (Mg^{2+}-PPi; with K) binding and/or hydrolysis, or Mg^{2+} or Ca^{2+} binding (with first D) (Rea *et al*. 1992*a*; Hedlund *et al*. 2006). EYYT motif is a highly conserved domain in higher plants and has been suggested to play a role in coupling PPi hydrolysis and may be related to H^+ translocation and H^+-PPase activity in plant vacuoles (Drozdowicz and Rea, 2001). All H^+-PPases contain a highly conserved GNTTAA domain that is considered to be an important H^+-PPase domain because it may be related to K^+-dependence (Wang *et al*. 2013). The GNTTAA domain is considered to be a type I/II marker, according to the first A site (Serrano *et al*. 2007). This site has 2 possible forms: the A form is the K^+-dependent H^+-PPase and the K form is the K^+-independent H^+-PPase (Belogurov and Lahti, 2002; Hirono *et al*. 2005; Serrano *et al*. 2007). The PdPPase sequence includes the GNTTAA domain, indicating that the ciliate has a type I K^+-dependent H^+-PPase. The dependence of V-PPase activity on K^+ ions has led to the suggestion of V-PPase-mediated physiological transport of K^+ ions into vacuoles (Baltscheffsky *et al*. 1999). The PPases best characterized so far lack an N-terminal SP, except those derived from *Trypanosoma* (Hill *et al*. 2000) and *Toxoplasma* (Drozdowicz *et al*. 2003). Although the exact role of this sequence is not well known, in the case of the V-H^+-PPase derived from *Toxoplasma gondii*, the presence of a putative N-terminal leader sequence suggests that this protein is processed in the endoplasmic reticulum and is moved to a location within the secretory pathway (Hill *et al*.

https://doi.org/10.1017/S0031182014001267 Published online by Cambridge University Press

2000; Drozdowicz *et al*. 2003). Like *T. cruzi* and *T. gondii*, *P. dicentrarchi* also has a 15-residue N-terminal SP. However, the *P. dicentrarchi* PdPPase also appears to be a mTP of 30 residues at the N-terminus. Most mTP signals are located at the N-terminus of the nascent amino acid chain (Emanuelsson *et al*. 2001). In both *Plasmodium falciparum* and *T. gondii*, the apicoplastical proteins contain an SP in conjuction with a transit peptide (TP) (Bender *et al*. 2003; Tonkin *et al*. 2006). The presence of mTP in the PPase sequence of *P. dicentrarchi* may be due to an error in bioinformatic program as it has been reported that many TPs show remarkable similarities to mTPs in terms of N-terminal position and amino acid composition (Staiger *et al*. 2009).

Most H^+-PPases are derived from 2 prototypes: the vacuolar H^+-PPase (V-PPase) from plants and the H^+-PPi synthase from the phototrophic bacterium *R. rubrum* (Rea *et al*. 1992*b*; Rea and Poole, 1993; Zhen *et al*. 1997). V-PPases are highly homologous, polytopic membrane proteins, composed of a single polypeptide ranging in size from 70 to 115 kDa (predicted) or 56 to 79 kDa (apparent) and by 14–17 α-helical transmembrane domains (Rea *et al*. 1992*b*; Drozdowicz and Rea, 2001; McIntosh and Vaidya, 2002). Variations in the predicted *Mr* (from the cDNA) and observed *Mr* (determined by SDS-PAGE) are well known in highly hydrophobic proteins such as V-PPases (Maddy, 1976; Zhen *et al*. 1997). In the present study, the *Mr* predicted from cDNA of PdPPase is of approximate size 62 kDa, which is roughly consistent with the apparent *Mr* obtained by a western blot with polyclonal antibodies produced by immunization with a DNA vaccine and a recombinant protein containing partial sequence HKAAVIGDTIGDPLK, which is a highly conserved motif among the V-PPases and which has been used to produce polyclonal antibodies for detecting V-PPases polypeptides (Kim *et al*. 1994; Zhen *et al*. 1997). The topological prediction sequence of the PdPPase shows the presence of 11 transmembrane spans, localizing the conserved domains characteristic of V-PPases in the first cytosolic loop.

Molecular and biochemical characterization of AVP2, a sequence-divergent V-PPase from *Arabidopsis*, provides the first indication that V-PPases from the same organisms can fall into 2 distinct categories (Drozdowicz *et al*. 2000) This phenomenon can also occur within the V-PPases of protozoan parasites such as *Plasmodium* (McIntosh *et al*. 2001). The data obtained here clearly demonstrate that the amino acid sequence of PdPPase (like sequences available in the public databases of H^+-PPases from other ciliates such as *T. thermophila*, *I. multifiliis* and *P. tetraurelia*) basically corresponds to the prototypical type I V-PPase, AVP1, derived from *A. thaliana* and that is contains most of the sequence motifs characteristic of this category of pump (Drozdowicz and Rea, 2001). Furthermore, the identification of 2 DNA fragments with different sequences in both *P. tetraurelia* and *T. pyriformis* indicated the occurrence of 2 paralogous H^+-PPase genes in these organisms (Pérez-Castiñeira *et al*. 2002*a*, *b*). Extensive protein database searches revealed that the deduced amino acid sequence of PdPPase is very similar to the ciliate H^+-PPase protein and fairly similar to H^+-PPase homologues of plants. Plant-like H^+-PPase genes were also found in free-living protozoa such as ciliates, heterotrophic euglenoids and heterokonts (Pérez-Castiñeira *et al*. 2002*a*, *b*).

In the western blots, V-PPase-specific antibodies produced against the peptide HKAAVIGDTIGDPLK (designated PAB_{HK}) recognized a V-PPase from the archaeon *P. aerophilum* cloned in a strain of *Sccharomyces cerevisiae* of size 64 kDa (Drozdowicz *et al*. 1999). The presence of V-PPase-like activity and PAB_{HK}-immunoreactive polypeptides in *P. falciparum*, *T. gondii*, *T. cruzi* and *Leishmania donovani* has also been demonstrated (Drozdowicz and Rea, 2001). In the present study, the polyclonal antibodies produced by genetic immunization and immunization with a recombinant protein containing this peptide also recognized a single band of about 62 kDa in western blots of membrane polypeptides of *P. dicentrarchi*.

In plants, V–H^+-PPases are present in the vacuole membrane (tonoplast) and also in the Golgi and plasma membrane (Rea and Poole, 1993; Long *et al*. 1995; Robinson *et al*. 1996). In trypanosomatids and apicomplexan parasites, as well as in the green alga *Chalmydomonas reinhardtii*, the slime mould *Dictyostelium discoideum* and the bacteria *Agrobacterium tumefaciens*, *R. rubrum* and *Syntrophus gentianae*, the V–H^+-PPase is located in acidocalcisomes and the plasma membrane (Schöcke and Schink, 1998; Luo *et al*. 1999; Rodrigues *et al*. 1999*a*, *b*; Docampo and Moreno, 2001; Martinez *et al*. 2002; Miranda *et al*. 2004; Seufferheld *et al*. 2004; Sen *et al*. 2009). Acidocalcisomes are acidic Ca^{2+}-storage organelles found in trypanosomatids and apicomplexan parasites and characterized by a high electron density and a high content of polyphosphates, calcium, magnesium, sodium and zinc (Docampo and Moreno, 1999). In ciliates, the cell membrane surrounds the entire cell including the cilia and below of cell membrane arranged the outer alveolar membrane and the inner alveolar membrane that circumscribe an alveolar space (Peck, 1977). In *P. dicentarchi*, the pattern of the alveolar ridges is of variable size that may reflect changes in osmotic or ionic concentrations across the membrane in response to the environment (Paramá *et al*. 2006). The results of the immunohistochemical analysis performed in the present study demonstrate that PdPPase is mainly located in the vacuole and in the alveolar membranes of the parasite.

https://doi.org/10.1017/S0031182014001267 Published online by Cambridge University Press

In *P. dicentrarchi*, PPi-driven H^+ transport, assayed by measuring changes in the absorbance of acridine orange (A_{495}–A_{530}), was blocked by NaF and by PPi analogues, as occurs in other V-PPases of parasitic protozoa such as *Trypanosoma brucei* (Rodrigues *et al*. 1999*b*). In general, 1,1-diphosphonates are potent type-specific inhibitors of V-PPase activity (Zhen *et al*. 1994). PPase analogue bisphosphonates are inhibitors of plant V/H^+-PPase and behave as competitive inhibitors of this enzyme (Gordon-Weeks *et al*. 1999; Szabo and Oldfield, 2001). In the present study, the bisphosphonate PAM significantly inhibited PPi-dependent H^+ translocation at a concentration of 0·1 mM and PdPPase gene expression at a concentration of 1 mM. Several studies emphasize the inhibitory effect of bisphosphonates, such as the pyrophosphatase isomerase and farnesyl pyrophosphatase synthase, on both the enzyme activity and gene expression of PPases (Van Beek *et al*. 1999; Montalvetti *et al*. 2003; Szajnman *et al*. 2012).

The apparent lack of V–H^+-PPase in mammalian cells makes this enzyme a potential target for specific chemotherapy (Luo *et al*. 1999; McIntosh and Vaidya, 2002). The most obvious class of potentially therapeutic compounds includes pyrophosphate analogues that act as competitive inhibitors of V-PPase (Baykov *et al*. 1993). Several bisphosphonates, including PAM, are already used for effective treatment of bone resorption, osteoporosis, Paget's disease, myeloma and bone metastases (Russell and Rogers, 1999). Bisphosphonates have been found to have an anti-parasitic effect on the trypanosomatids *Trypanosoma* and *Leishmania*, on the coccidians *Toxoplasma* and *Plasmodium*, on free-living amoebae such as *Dictyostelium*, and on amphizooic amoebae such as *Naegleria fowleri* (Rogers *et al*. 2000; Martin *et al*. 2001), all of which possess V-PPases. In addition to V-PPases, other PPases or phosphohydrolases may be targets for bisphosphonates, and the mechanisms of action may also be diverse; for example, it has been shown that some bisphosphonates can interfere with the isoprenoid pathway in the step catalysed by farnesyl diphosphate synthase, a major branching point in the mevalonate pathway (Rodan, 1998; Rogers *et al*. 2000). Bisphosphonates are also known to inhibit prenylation of small GTP-binding proteins that control cytoskeletal reorganization, vesicular fusion and apoptosis (Rodrigues *et al*. 2000). In the present study, the bisphosphonate PAM clearly inhibited *in vitro* growth of *P. dicentrarchi*.

In summary, because there is not yet any evidence for the existence of V-PPase in animal cells, molecular characterization of PdPPase is essential for structure–function analysis, and further development of new chemotherapeutic strategies is essential for the control of scuticociliatosis. The PdPPase sequence indicates that the enzyme is an authentic member of the family of V–H^+-PPases, as defined in plants and bacteria. Analysis of the role of PdPPase inhibitors in parasite survival will determine their suitability as a possible drug target.

ACKNOWLEDGEMENTS

This study was financially supported by grant numbers AGL2010-21219/ACU and AGL2011-29927-C02-01, from the Comisión Interministerial de Ciencia y Tecnología (CICYT; Spain), and grant number INCITE07/PX1203039ES from the Aquagenomics Project funded through the Consolider-Ingenio 2010 Programme by the Spanish Ministerio de Economía y Competitividad.

REFERENCES

Baltscheffsky, M., Schultz, A. and Baltscheffsky, H. (1999). H^+-PPases: a tightly membrane-bound family. *FEBS Letters* **457**, 527–533.

Baykov, A. A., Dubnova, E. B., Bakuleva, N. P., Evtushenko, O. A., Zhen, R. G. and Rea, P. A. (1993). Differential sensitivity of membrane-associated pyrophosphatases to inhibition by diphosphonates and fluoride delineates two classes of enzyme. *FEBS Letters* **327**, 199–202.

Baykov, A. A., Kasho, V. N., Bakuleva, N. P. and Rea, P. A. (1994). Oxygen exchange reactions catalyzed by vacuolar H(+)-translocating pyrophosphatase. Evidence for reversible formation of enzyme-bound pyrophosphate. *FEBS Letters* **350**, 323–327.

Baykov, A. A., Cooperman, B. S., Goldman, A. and Lahti, R. (1999). Cytoplasmic inorganic pyrophosphatase. *Progress in Molecular and Subcellular Biology* **23**, 127–150.

Belogurov, G. A. and Lahti, R. (2002). A lysine substitute for K + . A460K mutation eliminates K^+ dependence in H^+-pyrophosphatase of *Carboxydothermus hydrogenoformans*. *Journal of Biological Chemistry* **277**, 49651–49654.

Bender, A., van Dooren, G. G., Ralph, S. A., McFadden, G. I. and Scheider, G. (2003). Properties and prediction of mitochondrial transit peptides from *Plasmodium falciparum*. *Molecular and Biochemical Parasitology* **132**, 59–66.

Bradford, M. (1976). A rapid and sensitive method for the quantitation of microgram quantities of protein utilizing the principle of protein dye binding. *Analytical Biochemistry* **72**, 248.

Budiño, B., Lamas, J., Pata, M. P., Arranz, J. A., Sanmartín, M. L. and Leiro, J. (2011). Intraspecific variability in several isolates of *Philasterides dicentrarchi* (syn. *Miamiensis avidus*), a scuticociliate parasite of farmed turbot. *Veterinary Parasitology* **175**, 260–272.

Bustin, S. A., Benes, V., Garson, J. A., Hellemans, J., Huggett, J., Kubista, M., Mueller, R., Nolan, T., Pfaffl, M. W., Shipley, G. L., Vandesompele, J. and Wittwer, C. T. (2009). The MIQE guidelines: minimum information for publication of quantitative real-time PCR experiments. *Clinical Chemistry* **55**, 11–622.

Cooperman, B. S., Baykov, A. A. and Lathi, R. (1992). Evolutionary conservation of the active site of soluble inorganic pyrophosphatase. *Trends in Biochemical Sciences* **17**, 262–266.

Docampo, R. and Moreno, S. N. (1999). Acidocalcisome: a novel Ca^{2+} storage compartment in trypanosomatids and apicomplexan parasites. *Parasitology Today* **15**, 443–448.

Docampo, R. and Moreno, S. N. (2001). The acidocalcisome. *Molecular and Biochemical Parasitology* **114**, 151–159.

Docampo, R. and Moreno, S. N. (2008). The acidocalcisome as a target for chemotherapeutic agents in protozoan parasites. *Current Pharmaceutical Design* **14**, 882–888.

Drozdowicz, Y. M. and Rea, P. A. (2001). Vacuolar H^+-pyrophosphatase from the evolutionary backwaters into the mainstream. *Trends in Plant Science* **6**, 206–211.

Drozdowicz, Y. M., Lu, Y.-P., Patel, V., Fitz-Gibbon, S., Miller, J. H. and Rea, P. A. (1999). A thermostable vacuolar-type membrane pyrophosphatase from archeon *Pyrobaculum aerophilum*: implications for the origins of pyrophosphate-energized pumps. *FEBS Letters* **460**, 505–512.

Drozdowicz, Y. M., Kissinger, J. C. and Rea, P. A. (2000). AVP2, a sequence-divergent, K^+-insensitive H^+-translocating inorganic pyrophosphatase from *Arabidopsis*. *Plant Physiology* **23**, 353–362.

https://doi.org/10.1017/S0031182014001267 Published online by Cambridge University Press

Drozdowicz, Y. M., Shaw, M., Nishi, M., Striepen, B., Liwinski, H. A., Roos, D. S. and Rea, P. A. (2003). Isolation and characterization of TgVP1, a type I vacuolar H^+-translocating pyrophosphatase from *Toxoplasma gondii*. The dynamics of its subcellular localization and the cellular effects of a diphosphonate inhibitor. *Journal of Biological Chemistry* **278**, 1075–1085.

Emanuelsson, O., von Heijne, G. and Schneider, G. (2001). Analysis and prediction of mitochondrial targeting peptides. *Methods in Cell Biology* **65**, 175–187.

Gaxiola, R. A., Palmgreen, M. G. and Schumacher, K. (2007). Plant proton pumps. *FEBS Letters* **581**, 2204–2214.

Gordon-Weeks, R., Parmar, S., Davies, T. G. and Leigh, R. A. (1999). Structural aspects of the effectiveness of bisphosphonates as competitive inhibitors of the plant vacuolar proton-pumping pyrophosphatase. *Biochemical Journal* **337**, 373–377.

Hedlund, J., Cantoni, R., Baltscheffsky, M., Baltscheffsky, H. and Persson, B. (2006). Analysis of ancient sequence motifs in the H^+-PPase family. *FEBS Journal* **273**, 5183–5193.

Hill, J. E., Scott, D. A., Luo, S. and Docampo, R. (2000). Cloning and functional expression of a gene encoding a vacuolar-type proton-translocating pyrophosphatase from *Trypanosoma cruzi*. *Biochemical Journal* **351**, 281–288.

Hirono, M., Mimura, H., Nakanishi, Y. and Maeshima, M. (2005). Expression of functional *Streptomyces coelicolor* H^+-pyrophosphatase and characterization of its molecular properties. *Journal of Biochemistry* **138**, 183–191.

Iglesias, R., Paramá, A., Álvarez, M. F., Leiro, J., Fernández, J. and Sanmartín, M. L. (2001). *Philasterides dicentrarchi* (Ciliophora, Scuticociliatida) as the causative agent of scuticociliatosis in farmed turbot *Scophthalmus maximus* in Galicia (NW, Spain). *Diseases of Aquatic Organisms* **46**, 47–55.

Iglesias, R., Paramá, A., Álvarez, M. F., Leiro, J., Aja, C. and Sanmartín, M. L. (2003). *In vitro* growth requirements for the fish pathogen *Philasterides dicentrarchi* (Ciliophora, Scuticociliatida). *Veterinary Parasitology* **111**, 19–30.

Islam, M. K., Miyoshi, T., Yamada, M. and Tsuji, N. (2005). Pyrophosphatase of the roundworm *Ascaris suum* plays an essential role in the worm's molting and development. *Infection and Immunity* **73**, 1995–2004.

Karlsson, J. (1975). Membrane-bound potassium and magnesium ion-stimulated inorganic pyrophosphatase from roots and cotyledons of sugar beet (*Beta vulgaris* L). *Biochimica and Biophysica Acta* **399**, 356–363.

Kiefer, F., Arnold, K., Künzli, M., Bordoli, L. and Schwede, T. (2009). The SWISS-MODEL repository and associated resources. *Nucleic Acids Research* **37**, D387–D392.

Kim, E., Zhen, R.-G. and Rea, P. A. (1994). Heterologous expression of plant vacuolar pyrophosphatase in yeast demonstrates sufficiency of the substrate-binding subunit for proton transport. *Proceedings of the National Academy Sciences USA* **91**, 6128–6132.

Kornberg, A. (1962). On the metabolic significance of phosphorolytic and pyrophosphorolytic reactions. In *Horizons in Biochemistry* (ed. Kasha, M. and Pullman, B.), pp. 251–264. Academic Press, Inc., New York, USA.

Leiro, J., Siso, M. I. G., Iglesias, R., Ubeira, F. M. and Sanmartín, M. L. (2002). Mouse antibody response to a microsporidian parasite following inoculation with a gene coding for parasite ribosomal RNA. *Vaccine* **20**, 2648–2655.

Leiro, J., Arranz, J. A., Paramá, A., Álvarez, M. F. and Sanmartín, M. L. (2004). *In vitro* effects of the polyphenols resveratrol, mangiferin and (-)- epigallocatechin-3-gallate on the scuticociliate fish pathogen *Philasterides dicentrarchi*. *Diseases of Aquatic Organisms* **59**, 171–174.

Livak, K. J. and Schmittgen, T. D. (2001). Analysis of relative gene expression data using real-time quantitative PCR and the $2^{-\Delta\Delta Cq}$ method. *Methods* **25**, 402–408.

Long, A. R., Williams, L. E., Nelson, S. J. and Hall, J. L. (1995). Localization of membrane pyrophosphatase activity in *Ricinus communis* seedlings. *Journal of Plant Physiology* **146**, 629–638.

Luo, S., Marchesini, N., Moreno, S. N. J. and Docampo, R. (1999). A plant-like vacuolar H^+-pyrophosphatase in *Plasmodium falciparum*. *FEBS Letters* **460**, 217–220.

Maddy, A. H. (1976). A critical evaluation of the analysis of membrane proteins by polyacrylamide gel electrophoresis in the presence of dodecyl sulfate. *Journal of Theoretical Biology* **62**, 315–326.

Maeshima, M. (2000). Vacuolar H^+-pyrophosphatase. *Biochimica et Biophysica Acta* **1465**, 37–51.

Marchesini, N., Luo, S., Rodrigues, C. O., Moreno, S. N. and Docampo, R. (2000). Acidocalcisomes and vacuolar H^+-pyrophosphatase in malaria parasites. *Biochemical Journal* **347**, 243–253.

Martin, M. B., Grimley, J. S., Lewis, J. C., Health, H. T., Bailey, B. N., Kendrick, H., Yardley, V., Caldera, A., Lira, R., Urbina, J. A., Moreno, S. N., Docampo, R., Croft, S. L. and Oldfield, E. (2001). Bisphosphonates inhibit the growth of *Trypanosoma brucei*, *Trypanosoma cruzi*, *Leishmania donovani*, *Toxoplasma gondii*, and *Plasmodium falciparum*: a potential route to chemotherapy. *Journal of Medicinal Chemistry* **44**, 909–916.

Martinez, R., Wang, Y., Benaim, G., Benchimol, M., de Souza, W., Scott, D. A. and Docampo, R. (2002). A proton pumping pyrophosphatase in the Golgi apparatus and plasma membrane vesicles of *Trypanosoma cruzi*. *Molecular and Biochemical Parasitology* **120**, 205–213.

McIntosh, M. T. and Vaidya, A. B. (2002). Vacuolar type H^+ pumping pyrophosphatases of parasitic protozoa. *International Journal for Parasitology* **32**, 1–14.

McIntosh, M. T., Drozdowicz, Y. M., Laroiya, K., Rea, P. A. and Vaidya, A. B. (2001). Two classes of plant-like vacuolar-type H^+-pyrophosphatases in malaria parasites. *Molecular and Biochemical Parasitology* **114**, 183–195.

Miranda, K., Docampo, R., Grillo, O., Franzen, A., Attias, M., Vercesi, A., Plattner, H., Hentschel, J. and de Souza, W. (2004). Dynamics of polymorphism of acidocalcisomes in *Leishmania parasites*. *Histochemistry and Cell Biology* **1121**, 407–418.

Miranda, K., de Souza, W., Plattner, H., Hentschel, J., Kawazoe, U., Fang, J. and Moreno, S. N. (2008). Acidocalcisomes in apicomplexan parasites. *Experimental Parasitology* **118**, 2–9.

Montalvetti, A., Fernández, A., Sanders, J. M., Ghosh, S., Van Brussel, E., Oldfield, E. and Docampo, R. (2003). Farnesyl pyrophosphate synthase is an essential enzyme in *Trypanosoma brucei*. *In vitro* RNA interference and *in vivo* inhibition studies. *Journal of Biological Chemistry* **278**, 17075–17083.

Nakanishi, Y., Saijo, T., Wada, Y. and Maeshima, M. (2001). Mutagenic analysis of functional residues in putative substrate-binding site and acidic domains of vacuolar H^+-pyrophosphatase. *Journal of Biological Chemistry* **276**, 7654–7660.

Pace, D. A., Fang, J., Cintron, R., Docampo, M. D. and Moreno, S. N. (2011). Overexpression of a cytosolic pyrophosphatase (TgPPase) reveals a regulatory role of PP(i) in glycolysis for *Toxoplasma gondii*. *Biochemical Journal* **440**, 229–240.

Paramá, A., Arranz, J. A., Álvarez, M. F., Sanmartín, M. L. and Leiro, J. (2006). Ultrastructure and phylogeny of *Philasterides dicentrarchi* (Ciliophora: Scuticociliatia) from farmed turbot in NW Spain. *Parasitology* **132**, 555–564.

Peck, R. K. (1977). The ultrastructure of the somatic cortex of *Pseudomicrothorax dubius*: structure and function of the epiplasm in ciliated protozoa. *Journal of Cell Science* **25**, 367–385.

Pérez-Castiñeira, J. R., López-Marqués, R. L., Losada, M. and Serrano, A. (2001). A thermostable K(+)-stimulated vacuolar-type pyrophosphatase from the hyperthermophilic bacterium *Thermotoga maritima*. *FEBS Letters* **496**, 6–11.

Pérez-Castiñeira, J. R., López-Marqués, R. L., Villalba, J. M., Losada, M. and Serrano, A. (2002*a*). Functional complementation of yeast cytosolic pyrophosphatase by bacterial and plant H+-translocating pyrophosphatases. *Proceedings of the National Academy Sciences USA* **99**, 15914–15919.

Pérez-Castiñeira, J. R., Alvar, J., Ruiz-Pérez, L. M. and Serrano, A. (2002*b*). Evidence for a wide occurrence of proton-translocating pyrophosphatase genes in parasitic and free-living protozoa. *Biochemical and Biophysical Research Communications* **294**, 567–573.

Petel, G. and Genraud, M. (1989). Localization in sucrose gradients of pyrophosphatase activities in the microsomal fractions of Jerusalem artichoke (*Helianthus tuberosus* L.) tubers. *Journal of Plant Physiology* **134**, 466–470.

Piazzón, C., Lamas, J., Castro, R., Budiño, B., Cabaleiro, S., Sanmartín, M. L. and Leiro, J. (2008). Antigenic and cross-protection studies on two turbot scuticociliate isolates. *Fish and Shellfish Immunology* **25**, 417–424.

Quevillon, E., Silventoinen, V., Pillai, S., Harte, N., Mulder, N., Apweiler, R. and López, R. (2005). InterProScan: protein domains identifier. *Nucleic Acids Research* **33**, W116–W120.

Rea, P. A. and Poole, R. J. (1986). Chromatographic resolution of H^+-translocating pyrophosphatase from H^+-translocating ATPase of higher plant tonoplast. *Plant Physiology* **81**, 126–129.

Rea, P. A. and Poole, R. J. (1993). Vacuolar H^+-translocating pyrophosphatase. *Annual Review of Plant Physiology and Plant Molecular Biology* **44**, 157–180.

Rea, P. A., Britten, C. J. and Sarafian, V. (1992*a*). Common identity of substrate binding subunit of vacuolar H^+-translocating inorganic pyrophosphatase of higher plant cells. *Plant Physiology* **100**, 723–732.

Rea, P. A., Kim, Y., Sarafian, V., Poole, R. J., Davies, J. M. and Sanders, D. (1992*b*). Vacuolar H^+-translocating pyrophosphatases: a new category of ion translocase. *Trends in Biochemical Sciences* **17**, 348–353.

Robinson, D. G., Haschke, H. P., Hinz, G., Hoh, B., Maeshima, M. and Marty, F. (1996). Immunological detection of tonoplast polypeptides in the plasma membrane of pea cotyledons. *Planta* **198**, 95–103.

Rodan, G. A. (1998). Mechanisms of action of bisphosphonates. *Annual Review of Pharmacology and Toxicology* **38**, 375–388.

Rodrigues, C. O., Scott, D. A. and Docampo, R. (1999*a*). Presence of a vacuolar H + -pyrophosphatase in promastigotes of *Leishmania donovani* and its localization to a different compartment from the vacuolar H + -ATPase. *Biochemical Journal* **340**, 759–766.

Rodrigues, C. O., Scott, D. A. and Docampo, R. (1999*b*). Characterization of a vacuolar pyrophosphatase in *Trypanosoma brucei* and its localization to acidocalcisomes. *Molecular and Cellular Biology* **19**, 7712–7723.

Rodrigues, C. O., Scott, D. A., de Souza, W., Benchimol, M., Urbina, J. A., Oldfield, E. and Moreno, S. (2000). Vacuolar proton pyrophosphatase activity (PPi) in *Toxoplasma gondii* as possible chemotherapeutic targets. *Biochemical Journal* **349**, 737–745.

Rogers, M. J., Gordon, S., Benford, H. L., Coxon, F. P., Luckman, S. P., Monkkonen, J. and Frith, J. C. (2000). Cellular and molecular mechanisms of action of bisphosphonates. *Cancer* **88**, 2961–2978.

Russell, R. G. and Rogers, M. J. (1999). Bisphosphonates: from the laboratory to the clinic and back again. *Bone* **25**, 97–106.

Schöcke, L. and Schink, B. (1998). Membrane-bound proton-translocating pyrophosphatase of *Syntrophus gentianae*, a snytrophycally benzoate-degrading fermenting bacterium. *European Journal of Biochemistry* **256**, 589–594.

Scott, D. A., de Souza, W., Benchimol, M., Zhong, L., Lu, H. G., Moreno, S. N. and Docampo, R. (1998). Presence of a plant-like proton-pumping pyrophosphatase in acidocalcisomes of *Trypanosoma cruzi*. *Journal of Biological Chemistry* **273**, 22151–22158.

Sen, S. S., Bhuyan, N. R. and Bera, T. (2009). Characterization of plasma membrane bound inorganic pyrophosphatase from *Leishmania donovani* promastigotes and amastigotes. *African Health Sciences* **9**, 212–217.

Serrano, A., Pérez-Castiñeira, J. R., Baltscheffsky, M. and Baltscheffsky, H. (2007). H^+-PPases yesterday, today and tomorrow. *IUBMB Life* **59**, 76–83.

Seufferheld, M., Lea, C. R., Vieira, M., Oldfield, E. and Docampo, R. (2004). The H^+-pyrophosphatase of *Rhodospirillum rubrum* is predominantly located in polyphosphate-rich acidocalcisomes. *Journal of Biological Chemistry* **279**, 51193–51202.

Shen, H.-B. and Chou, K.-C. (2007). Signal-3L: a 3-layer approach for predicting signal peptides. *Biochemical and Biophysical Research Communications* **363**, 297–303.

Sievers, F., Wilm, A., Dineen, D., Gibson, T. J., Karplus, K., Li, W., López, R., McWilliam, H., Remmert, M., Söding, J., Thompson, J. D. and Higgins, D. G. (2011). Fast, scalable generation of high-quality protein multiple sequence alignments using ClustalOmega. *Molecular Systems Biology* **7**, 539.

Staiger, C., Hinneburg, A. and Klösgen, R. B. (2009). Diversity in degrees of freedom of mitochondrial transit peptides. *Molecular Biology and Evolution* **26**, 1773–1780.

Suzuki, Y., Yasunaga, T., Ohkura, R., Wakabayashi, T. and Sutoh, K. (1998). Swing of the lever arm of a myosin motor at the isomerization and phosphate-release steps. *Nature* **396**, 380–383.

Szabo, C. M. and Oldfield, E. (2001). An investigation of bisphosphonate inhibition of a vacuolar proton-pumping pyrophosphatase. *Biochemical and Biophysical Research Communications* **287**, 468–473.

Szajnman, S. H., Rosso, V. S., Malayil, L., Smith, A., Moreno, S. N., Docampo, R. and Rodriguez, J. B. (2012). 1-(Fluoroalkylidene)-1,1-bisphosphonic acids are potent and selective inhibitors of the enzymatic activity of *Toxoplasma gondii* farnesyl pyrophosphate synthase. *Organic and Biomolecular Chemistry* **10**, 1424–1433.

Takasu, A., Nakanishi, Y., Yamauchi, T. and Maeshima, M. (1997). Analysis of the substrate binding site and carboxyl terminal region of vacuolar H^+-pyrophosphatase of mung bean with peptide antibodies. *The Journal of Biochemistry* **122**, 883–889.

Tamura, K., Peterson, D., Peterson, N., Stecher, G., Nei, M. and Kumar, S. (2011). MEGA 5: molecular evolutionary genetics analysis using maximum likelihood, evolutionary distance, and maximum parsimony methods. *Molecular Biology and Evolution* **28**, 2731–2739.

Tonkin, C. J., Roos, D. S. and McFadden, G. I. (2006). N-terminal positively charged amino acids, but not their exact position, are important for apicoplast transit peptide fidelity in *Toxoplasma gondii*. *Molecular and Biochemical Parasitology* **150**, 192–200.

Van Beek, E., Pieterman, E., Cohen, L., Löwik, C. and Papapoulus, S. (1999). Nitrogen-containing bisphosphonates inhibit isopentenyl pyrophosphate isomerase/farnesyl pyrophosphate synthase activity with relative potencies corresponding to their antiresorptive potencies *in vitro* and *in vivo*. *Biochemical and Biophysical Research Communications* **255**, 491–494.

Wang, Y., Jin, S., Wang, M., Zhu, L. and Zhang, X. (2013). Isolation and characterization of a conserved domain in the Eremophyte H^+-PPase family. *PLoS ONE* **8**, e70099.

Woo, P. T. K. (1987). Immune response of fish to parasitic protozoa. *Trends in Parasitology* **3**, 186–188.

Xie, Y., Chen, S., Yan, Y., Zhang, Z., Li, D., Yu, H., Wang, C., Nong, X., Zhou, X., Gu, X., Wang, S., Peng, X. and Yang, G. (2013). Potential of recombinant inorganic pyrophosphatase antigen as a new vaccine candidate against *Baylisascaris schroederi* in mice. *Veterinary Research* **44**, 90.

Zdobnov, E. M. and Apweiler, R. (2001). InterProScan –- an intregration platform for the signature-recognition methods in InterPro. *Bioinformatics* **17**, 847–848.

Zhen, R. G., Baykov, A. A., Bakuleva, N. P. and Rea, P. A. (1994). Aminomethylenediphosphonate: a potent type-specific inhibitor of both plant and phototrophic bacterial H^+-pyrophosphatases. *Plant Physiology* **104**, 153–159.

Zhen, R. G., Kim, E. J. and Rea, P. (1997). The molecular and biochemical basis of pyrophosphatase-energized proton translocation at the vacuolar membrane. *Advances in Botanical Research* **25**, 297–337.

https://doi.org/10.1017/S0031182014001267 Published online by Cambridge University Press